



NRC Publications Archive Archives des publications du CNRC

Pipe-soil interaction analysis of jointed water mains

Rajani, B. B.; Zhan, C.; Kuraoka, S.

This publication could be one of several versions: author's original, accepted manuscript or the publisher's version. /
La version de cette publication peut être l'une des suivantes : la version prépublication de l'auteur, la version
acceptée du manuscrit ou la version de l'éditeur.

Publisher's version / Version de l'éditeur:

Canadian Geotechnical Journal, 33, 3, pp. 393-404, 1996-06-01

NRC Publications Record / Notice d'Archives des publications de CNRC:

<https://nrc-publications.canada.ca/eng/view/object/?id=fa6c029e-ebea-430c-b0b0-559449263975>

<https://publications-cnrc.canada.ca/fra/voir/objet/?id=fa6c029e-ebea-430c-b0b0-559449263975>

Access and use of this website and the material on it are subject to the Terms and Conditions set forth at

<https://nrc-publications.canada.ca/eng/copyright>

READ THESE TERMS AND CONDITIONS CAREFULLY BEFORE USING THIS WEBSITE.

L'accès à ce site Web et l'utilisation de son contenu sont assujettis aux conditions présentées dans le site

<https://publications-cnrc.canada.ca/fra/droits>

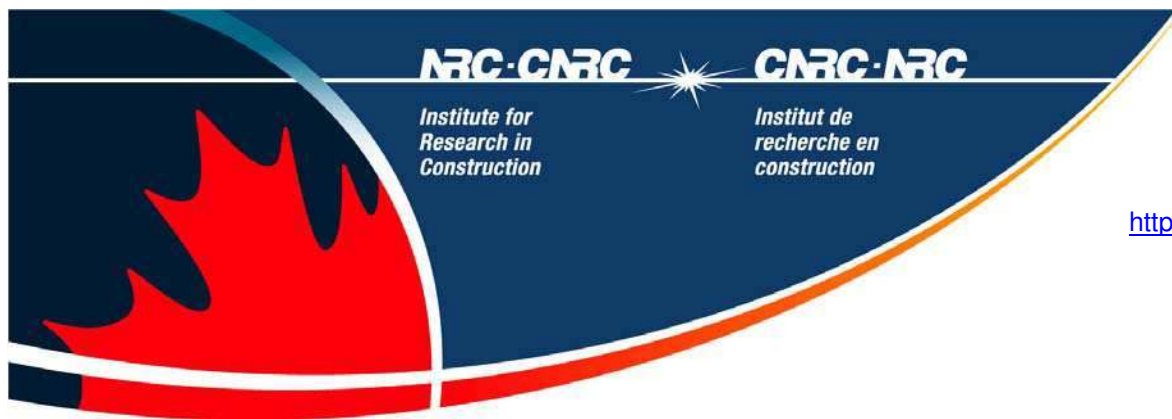
LISEZ CES CONDITIONS ATTENTIVEMENT AVANT D'UTILISER CE SITE WEB.

Questions? Contact the NRC Publications Archive team at

PublicationsArchive-ArchivesPublications@nrc-cnrc.gc.ca. If you wish to email the authors directly, please see the first page of the publication for their contact information.

Vous avez des questions? Nous pouvons vous aider. Pour communiquer directement avec un auteur, consultez la première page de la revue dans laquelle son article a été publié afin de trouver ses coordonnées. Si vous n'arrivez pas à les repérer, communiquez avec nous à PublicationsArchive-ArchivesPublications@nrc-cnrc.gc.ca.





<http://irc.nrc-cnrc.gc.ca>

Pipe-soil interaction analysis of jointed water mains

NRCC-39029

Rajani, B. ; Zhan, C. ; Kuraoka, S.

A version of this document is published in / Une version de ce document se trouve dans:
Canadian Geotechnical Journal, v. 33, no. 3, June 1996, pp. 393-404



National Research
Council Canada

Conseil national
de recherches Canada

Canada

Pipe-soil interaction analysis of jointed water mains

B. Rajani, C. Zhan, and S. Kuraoka

Abstract: Water mains are important lifelines of modern urban infrastructure. However, in most developed countries, the average life of these cast or ductile iron pipes approaches 50–75 years. In recent years, the disruption of water services as a consequence of water main breaks is on the rise in most Canadian cities. This paper describes the development of a simplified Winkler model to simulate the responses of a jointed water main subjected to differential temperature change and water pressure. The simplified Winkler model accounts for axial and radial restraints offered by the surrounding soil. In spite of its simplicity, the Winkler model is able to predict the overall response of strains and stresses, which confirms satisfactorily some of heuristic and documented observations on water main breaks.

Key words: water main breaks, pipe-soil interaction, temperature influence, Winkler model.

Résumé : Les conduites de distribution d'eau sont des composantes vitales de l'infrastructure urbaine. Cependant, dans la plupart des pays développés, la vie moyenne de ces tuyaux en fonte ou en acier ductile approchent 50 à 70 ans. Au cours des dernières années, l'interruption des services d'eau due aux bris des conduites de distribution a augmenté dans la plupart des villes canadiennes. Cet article décrit le développement d'un modèle simplifié Winkler pour simuler les réactions d'une conduite avec joints soumise à des différences de changement de température et de pression d'eau. Le modèle simplifié Winkler tient compte des restrictions axiales et radiales imposées par le sol environnant. En dépit de sa simplicité, le modèle Winkler peut prédire la réaction globale en contraintes et déformations qui confirme de façon satisfaisante certaines des observations heuristiques et documentées sur les bris des conduites de distribution.

Mots clés : bris de conduite de distribution d'eau, interaction tuyau-sol, influence de la température, modèle Winkler.

[Traduit par la rédaction]

Introduction

Water mains form an essential part of the lifeline systems of modern urban towns and cities. Cast iron pipes were extensively used to build water distribution systems from the early 1900s until ductile iron pipes were introduced in the 1970s. PVC water pipes were also introduced in Europe and North America during the 1970s, and recently, medium- and high-density polyethylene (MDPE and HDPE) have become alternative materials for the renewal of existing water mains. Asbestos-cement pipes, which are not used presently, were introduced in the 1930s. Most of the water mains installed during the first half of this century were either cast or ductile iron and currently have an average age of 50–75 years.

Statistics of the performance of water mains are typically expressed in terms of the frequency of breaks (events leading to the disruption of water service) per kilometre per year. A break frequency of greater than 5 breaks/100 km/year is undesirably high. Figure 1 shows the break

frequency (W.J. Borlase, private communication, 1993) for Winnipeg, Manitoba, which is typical of many cities in North America. Analyses of available data (e.g., Chambers 1994; Habibian 1994; Goulter and Kazemi 1989; Ciottoni 1985; Lackington and Large 1980) on the performance of water mains indicate that water main failure is influenced by seasonal climate, pipe diameter, and material type. A typical annual pattern of break rate shows (Fig. 2) that the peak in break frequency occurs during the period when ground temperatures are below normal. Similar studies (Needham and Howe 1981; Lochbaum 1993) on the performance of gas mains essentially reach the same conclusions. The data on water main breaks from all the mentioned studies can be summarized as follows:

(1) Studies of water main break histories for many cities indicate that a drop in seasonal temperatures is almost always followed by an increase in the number of breaks. Morris (1967) and Ciottoni (1983, 1985) suggest that break frequency in winter is at least twice as high as during summer.

(2) The frequency of breaks per kilometre per year increases (Fig. 3) with a decrease in pipe diameter. The high break frequency for small pipe sizes is often (Kettler and Goulter 1985) attributed to thinner pipe wall thickness, with a consequent reduction in the time to failure by corrosion.

Received May 10, 1995. Accepted December 10, 1995.

B. Rajani, C. Zhan, and S. Kuraoka. Institute for Research in Construction, National Research Council of Canada, Ottawa, ON K1A 0R6, Canada.

Fig. 1. History of water main breaks in Winnipeg, Manitoba.

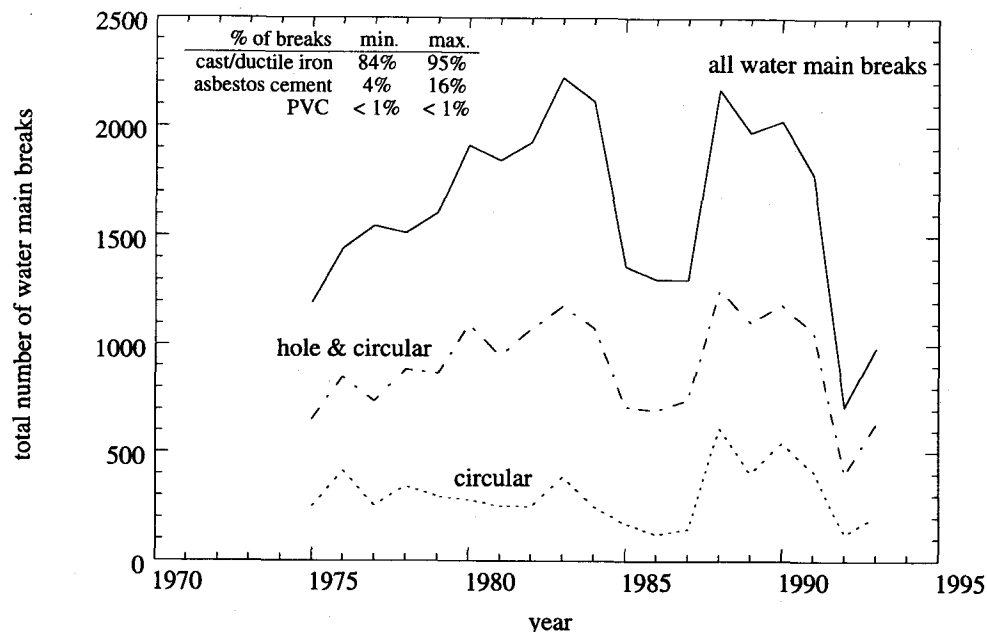
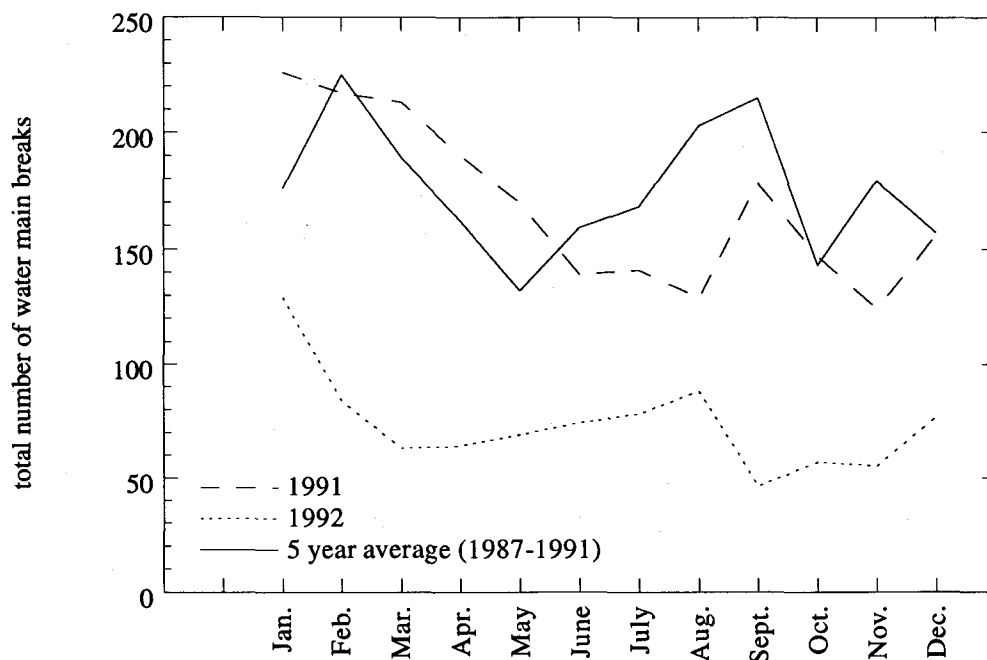


Fig. 2. Variation of break rate with pipe diameter.

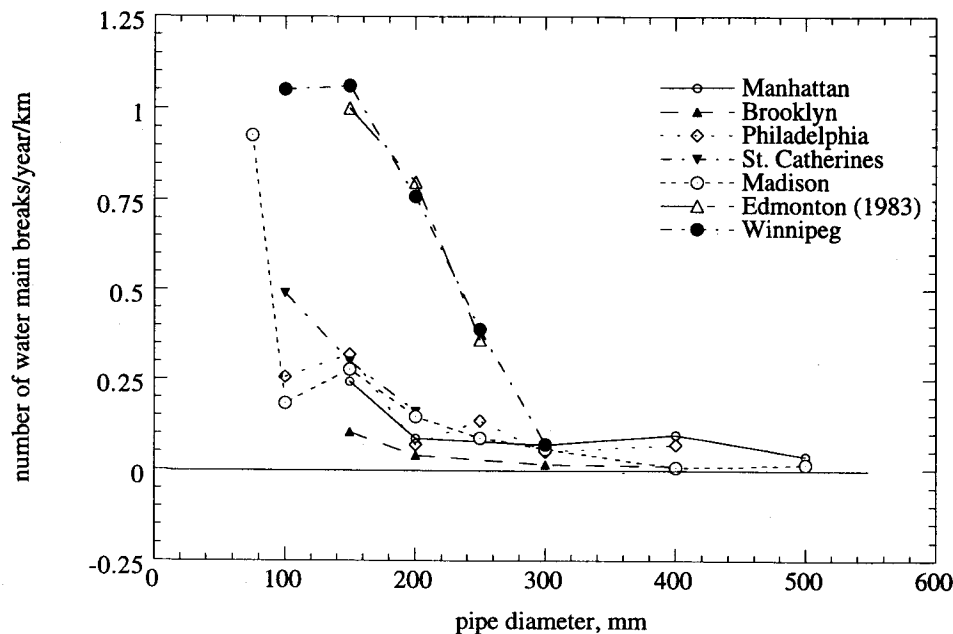


Modes of failure for water mains

Water main breaks occur in one of several modes of failure (Fig. 4): circular or circumferential break, longitudinal break or split, joint failure, holes due to corrosion and corporation cock failure. Breaks referred to as blow outs take place when the water mains are highly corroded and experience unusually high surge pressures. A circular break is evidence that a longitudinal tensile stress condition caused this type of failure. A longitudinal break is a result of circumferential or hoop stress and (or) in-plane bending action.

Longitudinal tensile stresses in water mains may be induced through one of several possible mechanisms. If the water mains were installed initially at a warm ambient temperature, they will contract (axially and to a minor extent circumferentially) upon a subsequent drop in water and ground temperatures. Buried water mains are restrained from movement by the frictional resistance between pipe and soil, with a corresponding development of axial stresses. Frictional resistance can increase over time if either the frictional angle or the normal load increase. Tensile stresses in the pipe can also be induced if clays with a

Fig. 3. Monthly variation of water main breaks in Winnipeg, Manitoba.



high montmorillonite mineral content undergo substantial volume change (Clark 1971) when subjected to seasonal wet and dry conditions. Morris (1967) reports that volumetric shrinkage for clays in Texas can be in the range of 14–40%. Flexural (bending) action due to inadequate bedding support or the swelling of underlying clays imposes additional longitudinal tensile stresses.

Large hoop stresses can arise either as a result of pressures exerted by an increase in volume when water freezes or large surge pressures. Kottmann (1994) has reported cases of longitudinal breaks in large-diameter grey cast iron, asbestos cement, and PVC low-pressure pipes as a consequence of air pocket formations during warm temperature conditions.

Although the statistics on the modes of failures vary from city to city, an average of 70% of water main breaks are circular and the other 30% are either longitudinal breaks, blow outs, or hydrant and service connection leaks. Consequently, the fact that the majority of the water mains fail in the circumferential mode and that these breaks primarily occur during the winter season suggest that axial pipe–soil interaction is the principal mechanism. As yet, an analytical procedure is not available that satisfactorily explains why extreme cold temperatures lead to an increase in the number of water main breaks. This paper describes a simple analytical pipe–soil interaction model that reflects the change in stress condition in water mains as a consequence of the change in water pressure and ground temperature. Field data from an instrumented PVC water main will be used to validate the proposed model in a subsequent paper.

A procedure for axial pipe–soil interaction analysis

Figure 5 shows the geometry of an idealized buried water main as well as the forces acting on an element of the water main. Pipes for water mains are usually available

in lengths of 6.1 m (20 ft) and are joined at the ends in a bell and spigot arrangement. A rubber gasket at the bell and spigot connections prevents leaks while permitting axial movement and slight rotation (3–4°); although some of the earlier water mains had lead caulked or bolted joints. The axial restraint, τ , on the pipe is a function of the normal force acting on the pipe and the frictional characteristics between the pipe material and surrounding backfill. In usual circumstances, the normal force is a result of vertical earth pressure, but it increases with water pressure and frost penetration (frost loading effects). The axial movement restraint, τ , can be expressed by the following relation:

$$[1] \quad \tau = k_s u$$

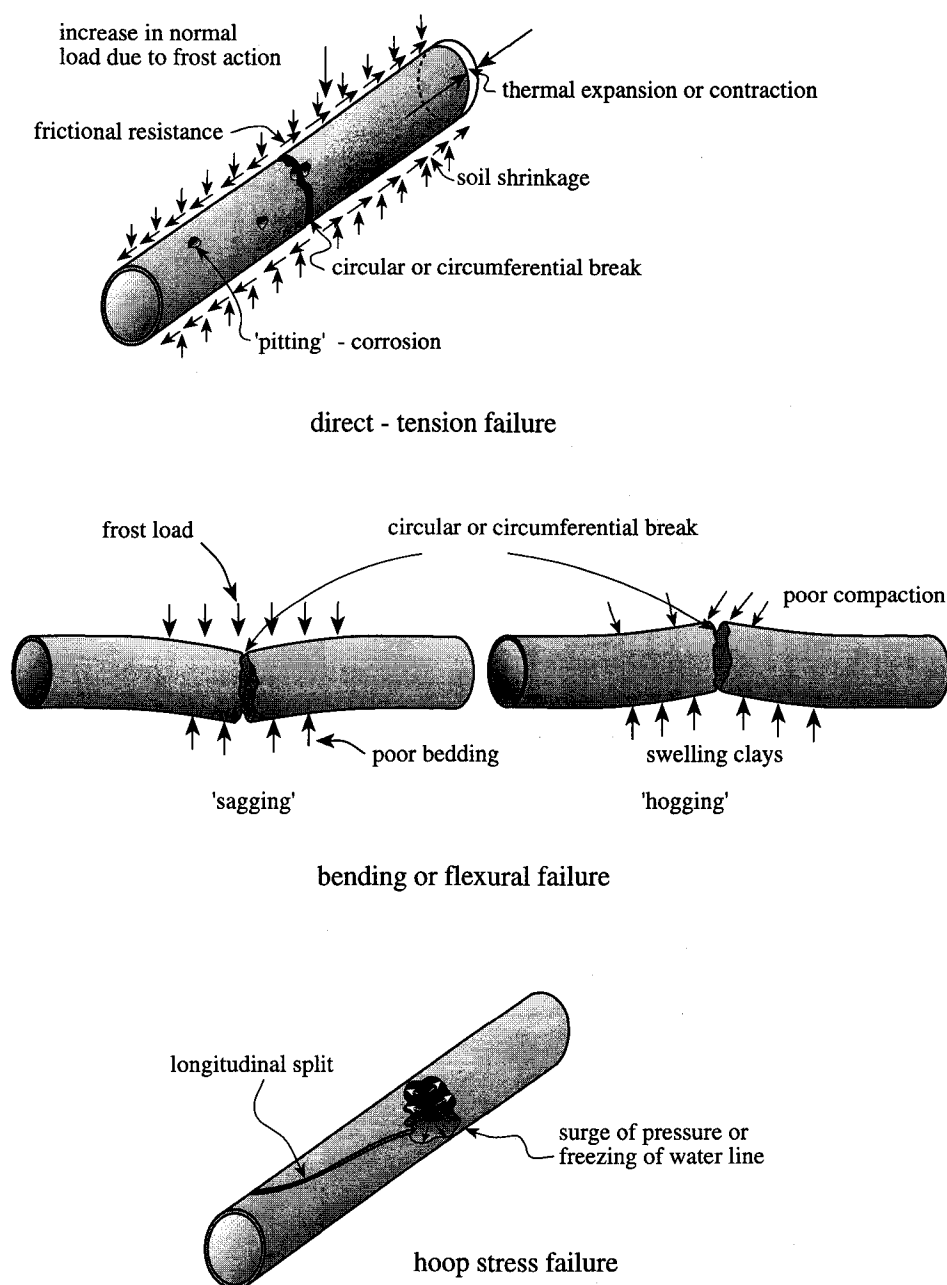
where u is the axial displacement and k_s is axial pipe–soil reaction modulus. The axial pipe–soil reaction modulus (Fig. 5) can be determined in one of several ways, either from elastic properties, as suggested by Scott (1981), or empirical relationships for sand and clay, as suggested by the Committee on Gas and Liquid Pipelines (1984). These relationships can be summarized as follows

$$[2] \quad k_s = \frac{G_s}{4(1 - \nu_s) \frac{D}{2}} \quad \text{elastic soil}$$

$$[3] \quad k_s = \frac{\alpha s_u}{u_y} \quad \text{clays}$$

$$[4] \quad k_s = \frac{0.5(\gamma_s H)(1 + K_o) \tan \delta}{u_y} \quad \text{sand}$$

where D is the external diameter of the pipe, G_s is the soil shear modulus, ν_s is the soil Poisson's ratio, α is the adhesion coefficient, s_u is the undrained shear strength of clays, u_y is the displacement required to develop ultimate axial resistance, γ_s is the submerged unit weight, H is the burial depth of water mains from surface to the centre line of

Fig. 4. Circular and longitudinal split failure modes of water mains.

the pipe, K_0 is the coefficient of active resistance at rest, and δ is the frictional angle between the pipe material and surrounding backfill. The Committee on Gas and Liquid Pipelines (1984) suggests that u_y for stiff clays is 5–10 mm (0.2–0.4 in.) and for loose to dense sands is 2.5–5 mm (0.1–0.2 in.). The increase in the normal force as a result of water pressure and "frost load" is reflected through parameters such as the adhesion factor (α) in clays and vertical earth pressure ($\gamma_s H$) in sand. Referring to Fig. 5, axial equilibrium for a pipe element dx can be expressed as

$$[5] \quad \frac{\partial P}{\partial x} - S\tau = 0 \quad \text{for} \quad u < u_y$$

where P is the axial load in the pipe, x is the axial coordinate,

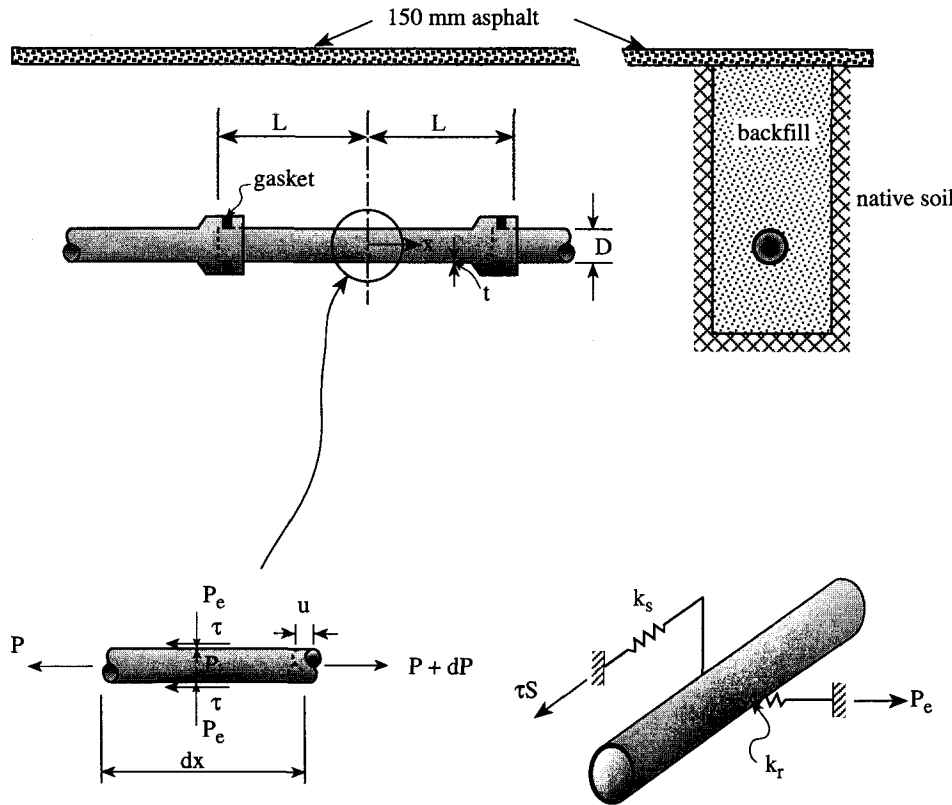
S is the external circumference of the pipe, and τ is the axial pipe–soil restraint described in [1]. The axial load, P , can be expressed in terms of axial stress and the cross-sectional area, i.e., $P = \sigma_x(\pi Dt)$, if the water pipe is assumed to be thin, i.e., $S = \pi D$, where D is the external diameter and t is the wall thickness. The equilibrium equation in [5] can be rewritten as

$$[6] \quad \frac{\partial \sigma_x}{\partial x} - \frac{k_s}{t} u = 0 \quad \text{for} \quad u < u_y$$

Axial strains

The effects of temperature need to be accounted for in addition to the water and external radial pressures to

Fig. 5. Geometry of jointed water mains.



determine the axial response from longitudinal restraint. If the response of the pipe remains within the elastic limit, the total axial strain, ϵ_x , is

$$[7] \quad \epsilon_x = \epsilon_x^f + \epsilon_x^w + \epsilon_x^T$$

where ϵ_x^f , ϵ_x^w , ϵ_x^T are strains corresponding to axial pipe resistance, water and earth radial pressures, and temperature, respectively. The axial strain corresponding to axial pipe stress is given by

$$[8] \quad \epsilon_x^f = \frac{\sigma_x}{E_p}$$

where E_p is the elastic pipe modulus. The axial strain, ϵ_x^w results from a combination of hoop stress ("stretching", σ_θ) and radial stress ("pinching", σ_r) as a consequence of internal water pressure, P_i , and external radial soil restraint, P_e . Contribution in the axial direction is diminished because of Poisson's ratio, ν , i.e.,

$$[9a] \quad \epsilon_x^w = -\nu \frac{\sigma_\theta}{E_p} - \nu \frac{\sigma_r}{E_p}$$

or

$$[9b] \quad \epsilon_x^w = -\nu \frac{D}{t} \frac{(P_i - P_e)}{2E_p} + \nu \frac{(P_i + P_e)}{2E_p}$$

The axial strain as a result of temperature change, ΔT , is given by

$$[10] \quad \epsilon_x^T = \alpha_p \Delta T$$

where α_p is the expansion coefficient of the pipe material. Substitution of the strain components in [8], [9], and [10] in [7] result in the following expression:

$$[11] \quad \epsilon_x = \frac{\sigma_x}{E_p} - \nu \frac{D}{t} \frac{(P_i - P_e)}{2E_p} + \nu \frac{(P_i + P_e)}{2E_p} + \alpha_p \Delta T$$

Axial strain can be alternatively expressed in terms of axial displacement, as $\partial u / \partial x$, and the differentiation of [11] with respect to the x coordinate leads to

$$[12] \quad \frac{\partial \sigma_x}{\partial x} = E_p \frac{\partial^2 u}{\partial x^2} + \frac{\nu}{2} \frac{D}{t} \left(\frac{\partial P_i}{\partial x} - \frac{\partial P_e}{\partial x} \right) - \frac{\nu}{2} \left(\frac{\partial P_i}{\partial x} + \frac{\partial P_e}{\partial x} \right)$$

assuming that temperature does not vary in the axial direction. A combination of [6] and [12] results in

$$[13] \quad E_p \frac{\partial^2 u}{\partial x^2} + \frac{\nu}{2} \frac{D}{t} \left(\frac{\partial P_i}{\partial x} - \frac{\partial P_e}{\partial x} \right) - \frac{\nu}{2} \left(\frac{\partial P_i}{\partial x} + \frac{\partial P_e}{\partial x} \right) - \frac{k_s}{t} u = 0$$

In usual circumstances, internal pressure, i.e., water pressure, does not vary with the x coordinate, consequently [13] reduces to

$$[14] \quad E_p \frac{\partial^2 u}{\partial x^2} - \frac{\nu}{2} \left(1 + \frac{D}{t} \right) \frac{\partial P_e}{\partial x} - \frac{k_s}{t} u = 0$$

Hoop strains

A combination of radial internal and external pressure, temperature change, and axial stress results in hoop strains as follows:

$$[15] \quad \epsilon_\theta = \epsilon_\theta^f + \epsilon_\theta^w + \epsilon_\theta^T$$

The above expression can be reduced to a form similar to that obtained for the axial strains, i.e.,

$$[16] \quad \epsilon_\theta = -\nu \frac{\sigma_x}{E_p} + \frac{D(P_i - P_e)}{t} + \nu \frac{(P_i + P_e)}{2E_p} + \alpha_p \Delta T$$

The hoop strain can be expressed as a function of radial displacement, i.e., $\epsilon_\theta = u_r/(D/2)$. The following equation for hoop strain results when the axial stress (σ_x) from [11] is substituted in [16]

$$[17] \quad \frac{u_r}{D} = \epsilon_\theta = -\nu \frac{\partial u}{\partial x} + (1 - \nu^2) \frac{D(P_i - P_e)}{t} + \nu(1 + \nu) \frac{(P_i + P_e)}{2E_p} + \alpha_p(1 + \nu)\Delta T$$

The radial displacement is constrained by the stiffness of the surrounding backfill and the force-displacement relation for a hole in an infinite medium is given by

$$[18] \quad P_e = k_r u_r = \frac{E_s}{\left(\frac{D}{2}\right)(1 + \nu_s)} u_r$$

where k_r and E_s are the radial stiffness and elastic modulus of the surrounding soil, respectively, and ν_s is the soil Poisson's ratio. The external radial pressure, P_e , can be determined as a function of internal pressure, temperature change, and axial pipe strain upon substitution of radial displacement from [17] into [18]

$$[19] \quad \beta_1 P_e = \beta_2 P_i - \frac{\nu E_s}{(1 + \nu_s)} \frac{\partial u}{\partial x} + \eta E_p \alpha_p \Delta T$$

where

$$\beta_1 = 1 + \eta(1 - \nu) \frac{D}{2t} - \eta \frac{\nu}{2}$$

$$\beta_2 = \eta(1 - \nu) \frac{D}{2t} + \eta \frac{\nu}{2}$$

and

$$\eta = \frac{E_s(1 + \nu)}{E_p(1 + \nu_s)}$$

Thus, eq. [19] describes the equilibrium condition in the radial direction.

The differentiation of [19] with respect to x and substitution of the resulting expression in [14] leads to

$$[20a] \quad \left[E_p + \frac{\nu^2 E_s}{2\beta_1(1 + \nu_s)} \left(1 + \frac{D}{t} \right) \right] \frac{\partial^2 u}{\partial x^2} - \frac{k_s}{t} u = 0$$

or

$$[20b] \quad \frac{\partial^2 u}{\partial x^2} - \frac{k_s}{\left[E_p + \frac{\nu^2 E_s}{2\beta_1(1 + \nu_s)} \left(1 + \frac{D}{t} \right) \right] t} u = 0$$

Equation [20b] has a form very similar to that of an axial bar embedded in an elastic medium (Hetényi 1974), which is

$$[21] \quad \frac{\partial^2 u}{\partial x^2} - \frac{Sk_s}{E_p A} u = 0$$

where S is the circumference of the bar as defined in [5] and A is cross-sectional area of the bar. If the bar is assumed to consist of a thin tube with diameter, D , and wall thickness, t , the solution for the differential eq. [20] can be expressed in terms of the characteristic length, $1/\gamma$. The parameter, γ , has dimensions L^{-1} and it is defined as

$$[22] \quad \gamma^2 = \frac{k_s}{\kappa E_p t} = \frac{k_s}{E_p t \left[1 + \frac{\nu^2 E_s}{2\beta_1(1 + \nu_s) E_p} \left(1 + \frac{D}{t} \right) \right]}$$

The parameter γ is the ratio of soil subgrade and pipe stiffnesses. The reciprocal of γ is the characteristic length of the pipe-soil system. Thus, the characteristic length is a measure of the elastic interaction between the pipe and the elastic foundation. The κ parameter reflects the influence of radial restraint on the axial pipe-soil interaction, and $\kappa = 1$ when no radial restraint is present. Solution to [20b] is

$$[23] \quad u = C_1 e^{-\gamma x} + C_2 e^{+\gamma x}$$

The constants in [23] can be found if the appropriate boundary conditions for the water mains problem are applied. Water mains consist of jointed pipes with individual lengths that have varied over the years from 5.4 m (18 ft) to 6.1 m (20 ft). If the individual pipe lengths are designated by $2L$ (Fig. 5), symmetry considerations for the axial movement of the pipe would indicate that the displacement at the mid-span of pipe length is zero, i.e.,

$$[24] \quad u(x = 0) = C_1 + C_2 = 0$$

The axial stresses at the ends of the pipe are zero, since the bell and spigot arrangement at the pipe ends permits free movement. The axial stress at any point along the pipe can be expressed by combining [11] and [19] to obtain

$$[25] \quad \sigma_x = \chi_1 E_p \frac{\partial u}{\partial x} + \chi_2 P_i - \chi_3 E_p \alpha_p \Delta T$$

where

$$\chi_1 = 1 + \frac{\nu^2}{2(1 + \nu_s)} \frac{E_s}{\beta_1 E_p} \left(1 + \frac{D}{t} \right)$$

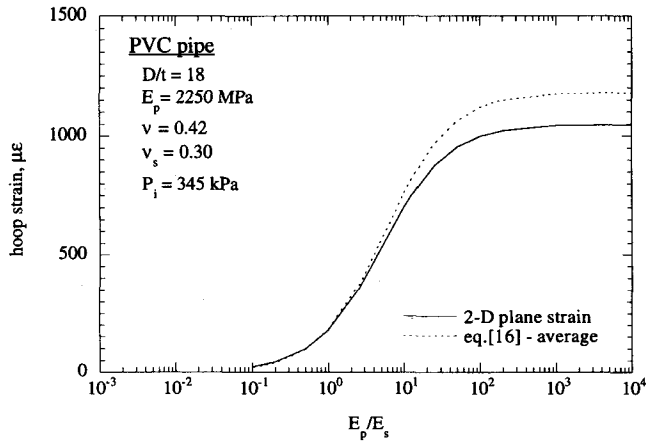
$$\chi_2 = \frac{\nu}{2} \left[\left(1 - \frac{\beta_2}{\beta_1} \right) \frac{D}{t} - \left(1 + \frac{\beta_2}{\beta_1} \right) \right]$$

and

$$\chi_3 = 1 + \frac{\nu \eta}{2\beta_1} \left(1 + \frac{D}{t} \right)$$

It is easy to appreciate from [25] that the three terms in the axial stress response correspond to the effects of axial pipe movement, internal water pressure, and temperature change, respectively. However, the effects of pipe-soil interaction of radial and axial restraint are reflected through the

Fig. 6. Comparison of exact and approximate hoop strains variations with E_p/E_s .



parameters, χ_1 , χ_2 , and χ_3 . Consequently, the constants C_1 and C_2 can be determined from [25] by substituting for the first derivative of axial displacement, u , evaluated at $x = L$ and let $\sigma_x = 0$. These constants can be expressed as follows

$$[26] \quad C_1 = -C_2 = \frac{(\chi_2 P_i - \chi_3 \alpha_p E_p \Delta T)}{\chi_1 \gamma E_p (e^{-\gamma L} + e^{+\gamma L})}$$

Once the constants, C_1 and C_2 , are known, axial and hoop strains can be determined from [11] and [16], respectively, as a function of the x coordinate, internal pressure, P_i , and temperature change, ΔT . Correspondingly, the axial stresses can be determined from [25].

The hoop stress for a thin-walled tube is given by

$$[27a] \quad \sigma_\theta = \frac{P_i - P_e}{2} \left(\frac{D}{t} \right)$$

or alternatively it can be expressed in the nondimensional form as

$$[27b] \quad \frac{P_i \left(\frac{D}{t} \right)}{\sigma_\theta} = \frac{2}{1 - \frac{P_e}{P_i}} = g \left\{ \frac{D}{t}, \frac{E_p}{E_s}, \nu_p, \nu_s, k_s, K \right\}$$

If P_e from [19] is substituted in [27b], the nondimensional response is primarily a function (g) of other nondimensional variables, such as the diameter-thickness ratio (D/t) and the pipe-soil elastic moduli ratio (E_p/E_s). In the case when there is no external restraint, i.e., pipe is not buried, $g = 2$; if the pipe is fully restrained radially, $P_i = P_e$, $g \rightarrow \infty$. Thus, an increase in the value of g is indicative of the radial restraint offered by the surrounding backfill.

The radial stress as expressed in [9b] is assumed to vary linearly, while the hoop stress is assumed to be constant across the wall thickness. The validity of these assumptions may be examined by comparing the hoop strain obtained from [16] and the exact hoop strain obtained by accounting for the effect of the wall thickness. The expression for exact hoop strain can be determined from Lamé's solution (Kuraoka et al. 1995) for a plane strain case with constant temperature, i.e., axial strain is zero. Thus, the exact hoop strain is computed at the centre of

Table 1. Reference data for typical ductile iron and PVC water mains, soil properties, and ground and pipe temperatures.

Pipe geometry	
External diameter, D	230 mm
Wall thickness, t (DI, PVC)	6.4 mm, 12.8 mm
Pipe length, $2L$	6.1 m
Ductile iron (DI)	
Elastic modulus, E_p	165 000 MPa
Ultimate tensile strength	290 MPa
Poisson's ratio, ν	0.28
Thermal coefficient, α_p	$11 \times 10^{-6}/^\circ\text{C}$
PVC	
Elastic modulus, E_p	2250 MPa
Ultimate tensile strength	48 MPa
Poisson's ratio, ν	0.42
Thermal coefficient, α_p	$79 \times 10^{-6}/^\circ\text{C}$
Operating conditions	
Water pressure, P_i	345 kPa (50 psi)
Soil properties	
Pipe-soil reaction modulus, k_s	125 MPa/m
Elastic modulus, E_s	100 MPa
Poisson's ratio, ν_s	0.3
Ground temperatures	
Installation temperature	24°C
Temperature amplitude, A^T	15°C
Annual mean temperature	15°C

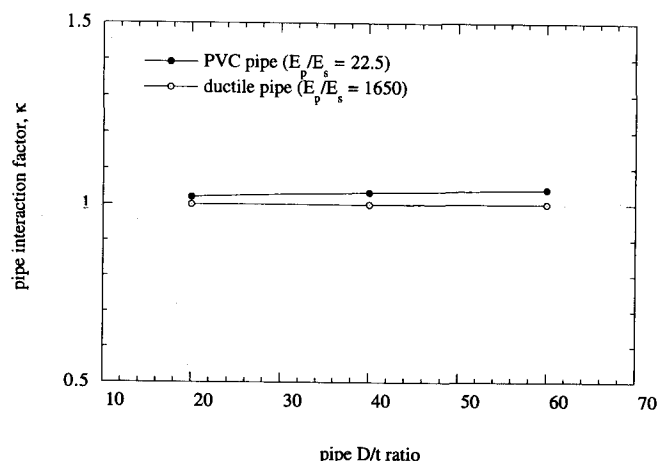
pipe wall using the data on pipe properties and water pressure given in Table 1 with a selected range of E_p/E_s while keeping E_p constant. The comparison between the two alternative methods for calculating hoop strain (Fig. 6) shows good agreement, which suggests that the assumptions made in the proposed analytical procedure are valid.

Sensitivity analysis

The response of jointed water main pipes obtained above can be used to conduct a sensitivity analysis in order to identify the influence of the key variables. The sensitivity analysis permits the confirmation of assertions that explains the modes of failure discussed earlier, i.e., (i) the water main break rate is likely to increase either during periods when the ground is extremely cold or when there is substantial drop in the water intake temperatures; (ii) water main breaks are more likely to take place in small diameter pipes than large diameter pipes; and (iii) surge pressures can have detrimental effects on the performance of water mains during cold temperature periods.

It is unfortunate that the stresses and strains cannot be expressed in nondimensional variables because, typically, the response is a function of many diverse variables. Consequently, for the purpose of the sensitivity analysis, a reference problem (Table 1) is selected and responses are determined by varying one key variable at a time. Axial pipe stress is reported rather than axial strain, since strain does not always lead to the development of stress. Axial

Fig. 7. Variation of pipe–soil axial interaction factor for different pipe materials.



pipe stress is maximum at mid-span, and its variation along the axial coordinate can be obtained from [23], [25], and [26].

A first step in this sensitivity analysis is to evaluate axial pipe–soil response as a function of the κ parameter introduced in [22]. The key variables involved in the κ parameter are D/t and E_p/E_s , whereas the Poisson's ratios for pipe and soil play minor influences. Figure 7 shows that while the interaction factor κ does not vary significantly with D/t ratio, there is not much difference in the interaction between PVC pipe and soil and that between ductile iron and soil.

Soil properties

As is often the case in soil–structure interaction analysis, soil properties are not as easily established as for the pipe. The three soil properties of interest in the axial pipe–soil responses are as follows: axial pipe–soil reaction modulus (k_s), soil elastic modulus (E_s), and Poisson's ratio (ν_s). The pipe–soil reaction modulus can be determined from basic soil properties as suggested in [2], [3], and [4] or from experimental studies. Biggar and Sego (1993) have conducted laboratory tests on model piles embedded in saline frozen soils from which reference values can be established. Variation in the axial pipe–soil reaction moduli, k_s , can be large even if soil properties are selected judiciously, as shown in Table 2. Soil temperatures can play a significant role in the behaviour of an embedded pipe as a result of reduction in moisture content.

Climatic conditions

Ground temperature during a 12 month period can be adequately represented as a function of time, \bar{t} , by

$$[28] \quad T(\bar{t}) = T_m + A^T \cos\left(\frac{2\pi\bar{t}}{365}\right)$$

where T_m is mean temperature and will vary according to the ground depth of interest, and A^T is the amplitude of temperature variation. In general, the mean temperature will increase with depth, and amplitude will depend on factors such as location and vegetation (ground cover).

Table 2. Range of values for axial pipe–soil reaction moduli.

Soil type	Axial pipe–soil stiffness (MPa/m)		
	Elastic response eq. [2]	CGL eqs. [3 and 4]	Biggar and Sego (1993)
Clay	20–600	2–10	600–1200
Sand	120–180	4–12	

Note: CGL, Committee on Gas and Liquid Pipelines.

Influence of axial pipe–soil reaction modulus (k_s)

Figure 8 shows that the axial stress response at half-span is strongly influenced by the axial pipe–soil restraint. The response of the pipe–soil interaction was determined for ductile iron water mains with the characteristics outlined in Table 1. All variables were kept constant except for the axial pipe–soil reaction modulus (k_s), which was varied within the range described in Table 2. Consequently, the determination of axial pipe–soil reaction modulus is an important issue, but values based on representative field or laboratory measurements are not available and can only be inferred from data available elsewhere, as explained in Table 2.

The stress condition discussed above refers to situations when the water mains have no defects. Stress concentration analysis (Ugural and Fenster 1985) shows the presence of a defect, such as that due to corrosion pits, can exacerbate the stress at the defect. This increase in stress is usually expressed in terms of the stress concentration factors, which can be as large as three for round pits (holes). In general, axial pipe–soil resistance increases with the roughness of the surface. Consequently, a corroded pipe with pits will induce more stress than a similar pipe with a smooth surface.

Influence of cold ground temperatures

As discussed previously, an increase in water main breaks is observed to occur during the colder season. The response of ductile iron water mains was determined by varying the ground temperatures through the variation of temperature amplitude, A^T . The magnitude of the amplitude reflects the extremes of seasonal temperatures. The response of a ductile iron pipe for a range of temperature amplitudes (Fig. 9) shows that axial stress changes by about 20% for each 5°C change in amplitude, A^T . Thus, this analysis demonstrates that cold ground temperatures can lead to an increase in circular water main breaks, and the additional stresses imposed on corroded water mains can be particularly damaging.

Role of pipe diameter

Many case studies (e.g., Ciottoni 1983, 1985; Kettler and Goulter 1985) have documented the fact that small diameter pipes are more likely to break than large diameter pipes. Kettler and Goulter (1985) attribute the high break frequency among small diameter pipes to reduced pipe wall thickness. Maximum response (Fig. 10) of ductile iron pipes of various sizes (Table 3) was obtained with the analytical model described above using the reference data

Fig. 8. Variation of axial stress in ductile iron pipe with pipe–soil reaction modulus (k_s).

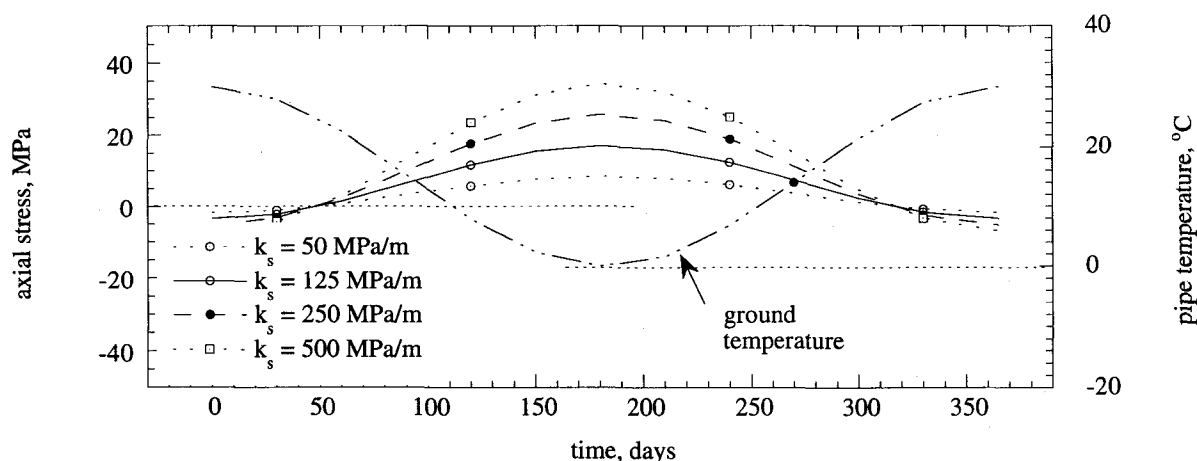
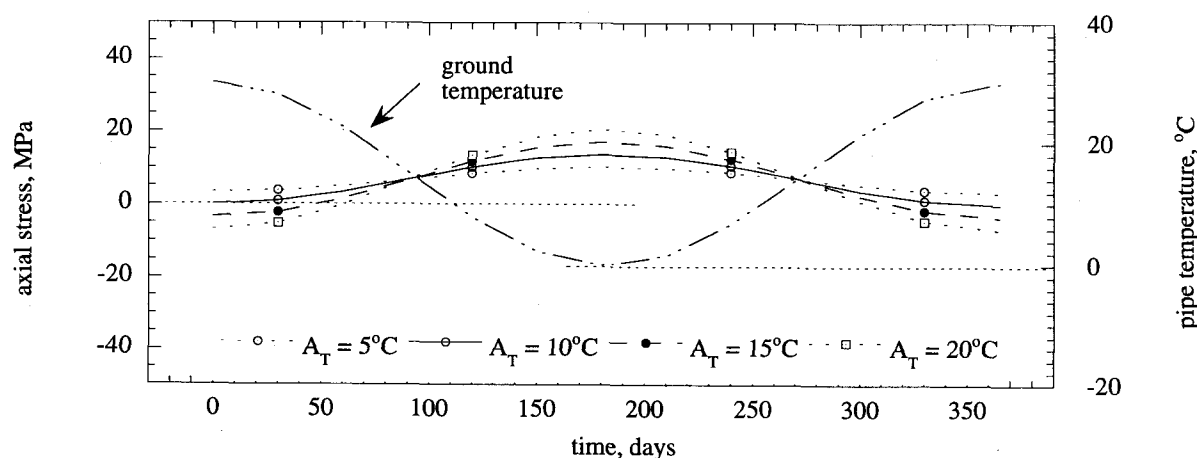


Fig. 9. Variation of axial stress in ductile iron pipe with changes in temperature extremes.



specified in Table 1. The difference in thickness between the smallest and largest pipe is 6 mm. Nonetheless, it is evident that the maximum axial stress induced in the water main, as a consequence of seasonal temperature extremes, is greater in small diameter pipes than in large diameter pipes, which confirms the water main statistical break data (Fig. 3).

PVC versus ductile iron water pipes

A question that must be asked is how does the behaviour of PVC pipes differ from that of ductile iron pipes? The two pipe materials have dramatically different elastic moduli as well as ultimate tensile strength, as is evident from the data in Table 1. While water mains of both materials are designed as flexible conduits, PVC pipe has to rely on the soil stiffness because of its reduced ring stiffness. However, since most water main breaks are circular, it is of interest to investigate how the behaviour of PVC and ductile iron pipe differs in response to extreme temperature changes.

For this analysis the axial pipe–soil reaction modulus (k_s) was not varied, since the influence of pipe material on the reaction modulus is not known, as discussed previously. It is most likely that the modulus is smaller for

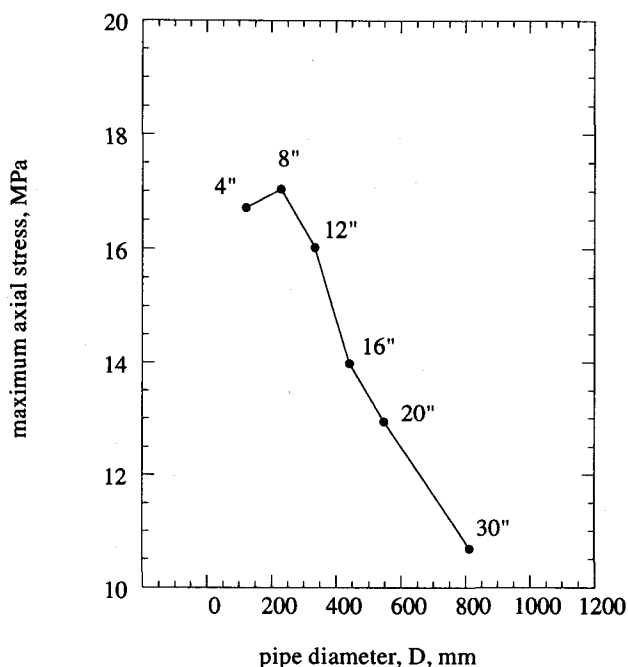
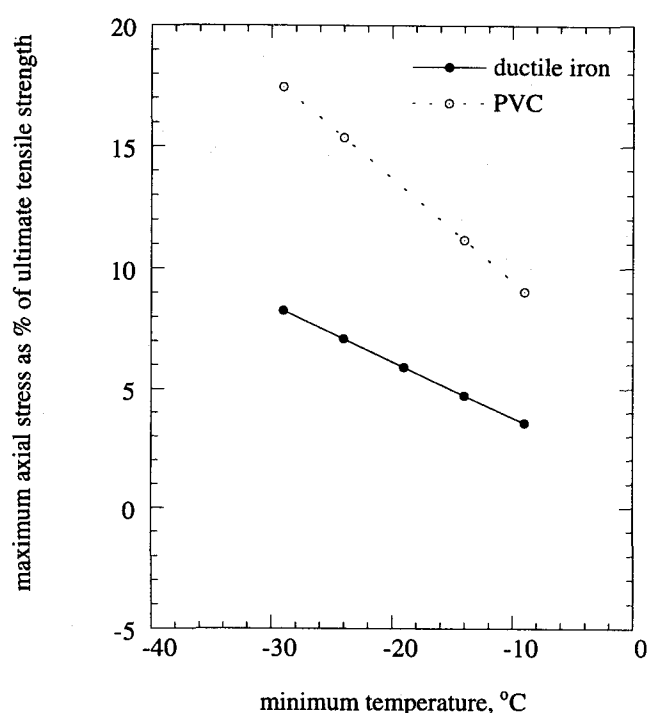
PVC–soil interface, since PVC pipe has a smoother finish than ductile iron pipe. The response of pipes (Fig. 11), in terms of the maximum axial stress, is rationalized with respect to the ultimate tensile strength of the pipe material. The difference in the response is primarily due to a dramatic contrast in the elastic moduli for ductile iron and PVC, i.e., the approximate difference is 80 times.

Surge pressures

The response of water mains to surge pressure is a major design consideration. The expected principal response to surge pressures is an increase in hoop stress, and this is mitigated by the soil stiffness of the backfill surrounding the pipe. The sensitivity of the nondimensional hoop stress response to the pipe–soil stiffness ratio can be determined if effects of temperature change are neglected. The results of such a sensitivity analysis are shown in Figs. 12 and 13 for ductile iron and PVC pipes. The sensitivity analysis clearly shows that as long as the pipe–soil elastic moduli ratio (E_p/E_s) is greater than 500, pipe response is such that it does not feel the radial restraint of the surrounding backfill. In general, a lower hoop stress develops in the buried pipe than if it had not been buried, and this is especially

Table 3. Dimensions for ductile and PVC water pipes.

Ductile iron				PVC			
Pressure class	Thickness t , mm	Diameter D , mm	D/t	Pressure class	Thickness t , mm	Diameter D , mm	D/t
350	6.35	121.9	19.20	200	8.71	121.95	14.00
350	6.35	229.9	36.20	150	12.78	229.87	17.99
350	7.11	335.3	47.14	100	13.41	335.28	25.00
350	8.64	442.0	51.18	100	12.09	495.30	40.97
350	9.65	548.6	56.84	100	13.39	548.64	40.99
350	12.45	812.8	65.31				

Fig. 10. Influence of pipe diameter on the maximum axial stress.**Fig. 11.** Influence of temperature extremes on the maximum axial stress for different pipe materials.

valid when the pipe-soil elastic moduli ratio (E_p/E_s) is less than 500. Elastic moduli for soils can increase significantly when temperatures decrease, as noted by Zhu and Carbee (1984), which means that frozen soils or backfill have a positive counteracting effect on the development of hoop stress in pipes. Thus, although surge pressures always lead to higher hoop stresses, cold ground temperatures do not appear to have a detrimental effect, compared with higher ground temperatures.

Conclusions

The pipe-soil interaction analytical model has been developed to provide a response of jointed water mains to changes in internal pressure and temperature. The model permits sensitivity analysis to identify key variables that play a major role in the overall behaviour of buried water mains. Although the analysis has relied on indirect estimates of the axial pipe-soil reaction modulus, a sensitivity analysis

of ductile iron and PVC water mains indicates that maximum axial stress increases substantially with a decrease in pipe size. This confirms the observation that small diameter water mains have a higher incidence of breaks even after taking into account their age and proportional representation in the water distribution network. The axial pipe-soil reaction modulus (k_s) has a significant influence on the response of pipe due to temperature changes, which illustrates the importance of obtaining reliable estimates of the reaction moduli for different pipe materials and soil types. The difference in the response for ductile iron and PVC pipes is primarily due to a dramatic contrast in the elastic moduli if the variation in the axial pipe-soil reaction modulus is disregarded. It was found that cold ground temperatures can lead to an increase in circular water main breaks and the additional stresses imposed on corroded water mains can be particularly damaging. The sensitivity

Fig. 12. Variation of hoop stress with D/t and E_p/E_s ratios for ductile iron pipes.

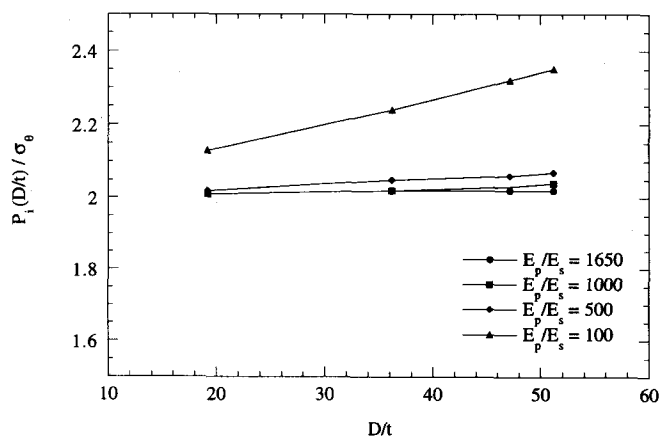
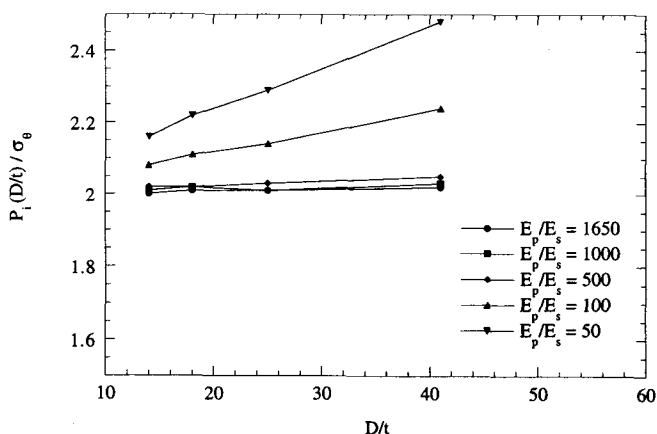


Fig. 13. Variation of hoop stress with D/t and E_p/E_s ratios for PVC pipes.



analysis clearly shows that as long as the pipe-soil elastic moduli ratio is greater than 500, pipe response to high surge pressures is such that it does not feel the radial restraint of the surrounding backfill. The frozen soils or backfill surrounding the buried pipe has a positive restraining effect and thus contributes towards the reduction of hoop stress.

The above discussion of axial or hoop stresses is always made in reference to intact pipe material, i.e., with no defects. Metallic pipes such as cast and ductile pipes develop pits as a result of corrosion, while PVC pipes can be easily scratched. Stress concentration analysis shows that these defects can cause the nominal stresses to increase by a factor of three in defective pipes, which shows that the presence of defects can only lead to higher stresses with a resulting increase in water main breaks.

References

- Biggar, K.W., and Sego, D.C. 1993. The strength and deformation behaviour of model adfreeze and grouted pipes in saline frozen soils. *Canadian Geotechnical Journal*, **30**: 319–337.

- Chambers, G.M. 1994. Reducing water utility costs in Winnipeg. *Proceedings of the Western Canada Water and Wastewater Association Conference*, Winnipeg, Man.
- Ciottoni, A.S. 1983. Computerized data management in determining causes of water main breaks: The Philadelphia case study. *Proceedings of the International Symposium on Urban Hydrology, Hydraulics and Sediment Control*, University of Kentucky, Lexington, Ky., pp. 323–329.
- Ciottoni, A.S. 1985. Updating the New York City water system. *Proceedings of the Specialty Conference on Infrastructure for Urban Growth*, pp. 69–77.
- Clark, C.M. 1971. Expansive-soil effect on buried pipe. *Journal of the American Water Works Association*, **63**: 424–427.
- Committee on Gas and Liquid Fuel Lifelines. 1984. Guidelines for the seismic design of oil and gas pipeline systems. American Society of Civil Engineers, New York.
- Goulter, I.C., and Kazemi, A. 1989. Analysis of water distribution pipe failure types in Winnipeg, Canada. *Journal of Transportation Engineering, ASCE*, **115**(2): 95–111.
- Habibian, A. 1994. Effects of temperature changes on water mains breaks. *Journal of Transportation Engineering, ASCE*, **120**(2): 312–321.
- Hetényi, M. 1974. Beams on elastic foundation. University of Michigan Press, Ann Arbor.
- Kettler, A.J., and Goulter, I.C. 1985. An analysis of pipe breakage in urban water distribution networks. *Canadian Journal of Civil Engineering*, **12**: 286–293.
- Kottmann, A. 1994. Pipe damage due to air pockets in low pressure piping. *Proceedings of the 2nd International Conference on Water Pipeline Systems*, Edinburgh, Scotland. Edited by D.S. Miller. pp. 41–52.
- Kuraoka, S., Rajani, B., and Zhan, C. 1995. Preliminary analysis of field tests of buried PVC water mains. *Proceedings, 1995 Annual Conference of the Canadian Society for Civil Engineering*, Ottawa, June 1–3, pp. 439–448.
- Lackington, D.W., and Large, J.M. 1980. The integrity of existing distribution systems. *Journal of the Institute of Water Engineers and Scientists*, **34**: 15–32.
- Lochbaum, B.S. 1993. PSE&G develop models to predict main breaks. *Pipeline and Gas Journal*, **220**: 20–27.
- Morris, R.E. 1967. Principal causes and remedies of water main breaks. *Journal of American Water Works Association*, **54**: 782–798.
- Needham, D., and Howe, M. 1981. Why gas mains fail. Part 1. *Pipe Line Industry*, **55**: 47–50.
- Scott, R.F. 1981. Foundation analysis. Prentice Hall, New Jersey, N.Y.
- Ugural, A.C., and Fenster, S.K. 1985. Advanced strength of materials and applied elasticity. Elsevier, New York.
- Zhu, Y., and Carbee, D.L. 1984. Uniaxial compressive strength of frozen silt under constant deformation rates. *Cold Regions Science Technology*, **9**: 3–15.

List of symbols

- | | |
|------------|---------------------------------------------------------------------|
| A | cross-sectional area of pipe or bar |
| A^T | amplitude of temperature variation |
| C_1, C_2 | constants |
| D | external pipe diameter |
| E_p | elastic pipe modulus |
| E_s | soil elastic modulus |
| G_s | soil shear modulus |
| H | burial depth of water mains from surface to the centre line of pipe |
| k_r | radial soil stiffnesses |
| k_s | axial pipe-soil reaction modulus |

K_o	coefficient of active resistance at rest	α_p	expansion coefficient of pipe material
L	half pipe length	$\eta, \chi_1, \chi_2, \chi_3$	constants
s_u	undrained shear strength of clays	δ	soil-pipe frictional angle
P	axial load acting on pipe	ΔT	temperature change
P_i	internal water pressure	$\epsilon_x^f, \epsilon_x^w, \epsilon_x^T$	strains corresponding to axial pipe resistance, water, and earth radial pressures, and temperature
P_e	external radial soil restraint		
S	external circumference of pipe	κ	parameter reflecting the influence of radial restraint on the axial pipe-soil interaction
t	pipe wall thickness	γ	1/elastic characteristic length
T	temperature in Celsius	γ_s	soil submerged unit weight
T_m	mean temperature	ν	Poisson's ratio for pipe
\bar{t}	time	ν_s	soil Poisson's ratio
u	axial displacement	$\sigma_x, \sigma_\theta, \sigma_r$	axial, hoop, and radial pipe stress
u_y	displacement required to develop ultimate axial resistance	τ	axial pipe-soil resistance
x	longitudinal coordinate axis		
α	soil-pipe adhesion coefficient		